Anal Bioanal Chem (2012) 402:405–412
DOI 10.1007/s00216-011-5497-y

ORIGINAL PAPER

The aromatic peroxygenase from *Marasmius rutola*—a new enzyme for biosensor applications

Aysu Yarman · Glenn Gröbe · Bettina Neumann · Mathias Kinne · Nenad Gajovic-Eichelmann · Ulla Wollenberger · Martin Hofrichter · René Ullrich · Katrin Scheibner · Frieder W. Scheller

Received: 3 August 2011 / Revised: 17 September 2011 / Accepted: 11 October 2011 / Published online: 25 October 2011

Abstract The aromatic peroxygenase (APO; EC 1.11.2.1) from the agraric basidomycete *Marasmius rotula* (*Mro*APO) immobilized at the chitosan-capped gold-nanoparticle-modified glassy carbon electrode displayed a pair of redox peaks with a midpoint potential of −278.5 mV vs. AgCl/AgCl (1 M KCl) for the Fe^{2+}/Fe^{3+} redox couple of the heme-thiolate-containing protein. *Mro*APO oxidizes aromatic substrates such as aniline, *p*-aminophenol, hydroquinone, resorcinol, catechol, and paracetamol by means of hydrogen peroxide. The substrate spectrum overlaps with those of cytochrome P450s and plant peroxidases which are relevant in environmental analysis and drug monitoring. In *M. rotula* peroxygenase-based enzyme electrodes, the signal is generated by the reduction of electrode-active reaction products (e.g., *p*-benzoquinone and *p*-quinoneimine) with electroenzymatic recycling of the analyte. In these enzyme electrodes, the signal reflects the conversion of all substrates thus representing an overall parameter in complex media. The performance of these sensors and their further development are discussed.

Keywords Unspecific peroxygenase · Cytochrome P450 · Biosensors · Phenolic substances

Published in the *10th Anniversary Issue*.

Aysu Yarman and Glenn Gröbe contributed equally to this work.

A. Yarman · B. Neumann · N. Gajovic-Eichelmann · F. W. Scheller
Fraunhofer Institute for Biomedical Engineering IBMT, 14476 Potsdam, Germany

G. Gröbe · K. Scheibner
Department of Biotechnology, Lausitz University of Applied Sciences, 01968 Senftenberg, Germany

M. Kinne · M. Hofrichter · R. Ullrich
Unit of Environmental Biotechnology, International Graduate School of Zittau, 0276 Zittau, Germany

U. Wollenberger · F. W. Scheller (✉)
Institute of Biochemistry and Biology, University of Potsdam Karl-Liebknecht-Str. 24–25, 14476 Golm, Germany
e-mail: fschell@uni-potsdam.de

Introduction

The high specificity of biological macromolecules like enzymes and antibodies has been exploited for more than 50 years in clinical analysis, food control, and environmental analysis. Based on the technologies of laboratory analyzers and test strips, a new generation of analytical tools, biosensors, and biochips has been created [1–6].

Enzymes of the cytochrome P450s (P450) family act on more than 90% of all drugs currently on the market. Therefore, P450s have been used as recognition elements in drug sensors. The P450 enzymes contain an iron protoporphyrin IX moiety with cysteine as the fifth ligand. The catalytic cycle of most P450s requires electron supply to the heme iron in the presence of oxygen from NAD(P)H. Usage of hydrogen peroxide as source of oxygen for the conversion of the analyte would circumvent the supply with NAD(P)H. Peroxygenases catalyzing oxygen transfer reactions similar to the "peroxide shunt" of cytochrome P450s transfer an oxygen atom from peroxide to a large variety of substrates and, in dependence of the substrate, they can work selectively and under ambient conditions [7, 8]. Extracellular biocatalysts of the heme peroxidase type are

secretory proteins and hence relatively stable, they have the same prosthetic group as P450s and form similar activated oxo-intermediates [9].

After the aromatic peroxygenases*[1] (APOs; EC 1.11.2.1) of the agaric basidiomycetes *Agrocybe aegerita* and *Coprinellus radians* [10], the peroxygenase of the Pinwheel mushroom (*Marasmius rotula* aromatic peroxygenase= *Mro*APO) is the third characterized enzyme of this type and the first one that can be produced in high yields [11].

The proteins of *Aae*APO and *Mro*APO show only 65% amino acid sequence homology, and accordingly, they differ to some extent in their physical and catalytic properties, e.g., in molecular weight, isoelectric point, extent of glycosylation, and kinetic data for particular substrates such as phenols, alkylbenzenes, or naphthalene derivatives. Furthermore, *Aae*APO has a haloperoxidase activity (i.e., it brominates phenol in the presence of bromide), which is lacking in *Mro*APO.

Recently, we initiated the application of APOs as recognition elements in biosensors for aromatic substances. The *Aae*APO sensor allowed the measurement of naphthalene, *p*-nitrophenol, aniline, and *p*-aminophenol in the lower micromolar range [12].

In this paper, we present an enzyme electrode for the determination of aromatic substances using *Mro*APO as the biocatalyst. To compare the potential of both peroxygenases, we used the same immobilization method for the aromatic peroxygenases from *Agerocybe aegerita* (*Aae*APO) and *Marasmius rotola* (*Mro*APO).

The preparation, electrochemical characterization, and immobilization of this peroxygenase as well as the development of a peroxide-dependent sensor are described.

Experimental

Chemicals

Hydrogen peroxide (H_2O_2, 30%), $HAuCl_4$, chitosan (CH; 85% deacetylated), anilinium hydrochloride, L-DOPA, *p*-nitrophenol, resorcinol, and paracetamol were purchased from Sigma (Steinheim, Germany) and *p*-aminophenol (pAP), hydroquinone, and catechol from Fluka (Germany).

All reagents were of analytical grade and used without further purification.

[1] In analogy to most P450s that are described in the EC system as unspecific monooxygenase (EC 1.14.14.1), fungal peroxygenases have been registered there under the systematic name unspecific peroxygenase (www.chem.qmul.ac.uk/iubmb/enzyme/EC1/11/2/1.html)

Organism

M. rotula (Scop.) Fr. was isolated from fruiting bodies near Senftenberg (Brandenburg, Germany) and deposited in the German Collection of Microorganisms and Cell Cultures (*Deutsche Sammlung für Mikroorganismen und Zellkulturen*) Braunschweig under DSMZ 2503 [11]. Fungal stock cultures were grown in culture slants on 2% malt extract agar (MA) at 24 °C and stored at 4 °C in the dark. Pre-cultures used as inoculation material for liquid cultures were obtained from 10-day-old overgrown MA plates.

Enzyme assay

Peroxygenase activity was routinely measured by following the oxidation of veratryl alcohol (3,4-dimethoxybenzyl alcohol) into veratraldehyde (3,4-dimethoxybenzaldehyde) at 310 nm (ε_{310}, 9,300 M^{-1} cm^{-1}) in McIlvaine buffer (Na citrate/phosphate, 50 mM) at pH 5.5 (modified according to Ref. [13]). The reaction was started by addition of 2 mM H_2O_2 and continued over 20–30 s.

Enzyme production, purification, and characterization

A complex growth medium containing glucose (4.2%), soybean peptone (4.8%), and yeast extract (0.45%) was used to produce *Mro*APO in liquid culture (culture flasks or stirred tank bioreactors) [11]. The protein was secreted in concentrations up to 450 mg L^{-1} (corresponding to approx. 40,000 UL^{-1} based on the veratryl alcohol assay).The culture liquid was filtered, frozen at −80 °C, rethawed, and centrifuged to remove polysaccharides [13]. This crude extract was concentrated by ultrafiltration and purified by five chromatographic steps using a fast liquid protein chromatography system and different anion exchangers as well as a size exclusion chromatography [11]. The specific activity of the purified enzyme was 77 Umg^{-1} (veratryl alcohol assay), and it was used for the electrochemical and physical characterization.

The latter revealed a molecular weight of 32 kDa (by SDS-PAGE) and isoelectric points (p*I*s) between 4.97 and 5.27 (three bands with the major one at pH 5.27). The major isoform was deglycosylated, which reduced the molecular weight of *Mro*APO by 5 kDa, i.e., the mature enzyme has a carbohydrate content of 16% [11].

Preparation of electrodes and electrochemical measurements

Gold nanoparticles-capped with chitosan (AuNP-CH) were prepared according to the method developed by Bonnard et al. Briefly, 80 μL of 4% of $HAuCl_4$ acid solution in water

was added to 50-mL distilled water containing 250 μl of 0.2 M K_2CO_3 in ice bath and stirred continuously; 500 μL of 0.5 mg/mL sodium borohydride solution was added stepwise and stirring continued for 20 min. Four volumes of these particles were mixed with 1 vol. of 1% (*w*/*v*) chitosan solution in 1% acetic acid [14].

The glassy carbon electrodes (GCEs) were polished with a wet slurry of 1.0, 0.3, and 0.05 μM Al_2O_3, respectively, and cleaned with Milli-Q water by sonication immediately before each use.

Modification of the electrodes followed the method reported elsewhere [12, 15]. *Mro*APO-AuNP-CH-modified electrodes were prepared by dropping 10 μL of a 1:1 mixture of *Mro*APO stock solution and AuNP-CH solution onto the freshly polished GCE surface (*Mro*APO-AuNP-CH/GCE). For control experiments, electrodes without enzymes or without gold nanoparticles were prepared. All modified electrodes were dried at 4 °C overnight and rinsed thoroughly with Milli-Q water prior to use.

Electrochemical measurements were performed in a stirred electrochemical cell (2 mL volume) with a three-electrode configuration. A glassy carbon disk electrode (3 mm in diameter) was used as the working electrode, an Ag/AgCl (in 1 M KCl solution) electrode was the reference electrode, and the platinum wire served as counter electrode.

Experiments for the direct electron transfer and square-wave voltammetry (SWV) were performed in an anaerobic chamber (COY; USA) using a GAMRY potentiostat. Cyclic voltammograms (CVs) were recorded in phosphate buffer (10 mM, pH 7) and scanned from −600 to 0 mV vs. Ag/AgCl (in 1 M KCl) with different scan rates.

Amperometric measurements were performed under aerobic conditions in 10 mM phosphate buffer at pH 7. A working potential of 0 mV vs. Ag/AgCl (in 1 M KCl) was applied for the reduction of the reaction products and of 200 mV vs. Ag/AgCl (in 1 M KCl) for the oxidation of the phenolic substances was applied, respectively. After baseline stabilization had occurred, 50 μM H_2O_2 was added. Current was recorded after the addition of substances into the reaction chamber as a function of time.

All the experiments were carried out at room temperature.

Conversion studies and HPLC

The enzymatic conversion of aniline, *p*-aminophenol, hydroquinone, and paracetamol was performed in 1.5 mL reaction vials containing 50 mM potassium phosphate buffer (pH 7.0), 500 μM substrate, and 1 U *Mro*APO (0.31 μM). The reaction was started by the addition of H_2O_2 (100 μM). The entire reaction volume was 200 μl.

The metabolites were analyzed by HPLC/MS using an Agilent® 1200 system (Waldbronn, Germany) equipped with a diode array detector, an electrospray ionization mass spectrometer and a Luna reversed phase C18 (2) column (4.6×125 mm, 5 μm; Phenomenex, Aschaffenburg, Germany). For analysis, a gradient separation was applied from 5% to 100% acetonitrile (0–5 min, 5%; 5–30 min, 5–100%) in 0.1% ammonium formate buffer (pH 7) at a flow rate of 1 mL min^{-1}. Products were identified relative to authentic standards, based on their retention times, UV absorption spectra, and $[M+H]^+$ ions. Eluted substances were recorded at 254 nm and identified/quantified by means of authentic standards and GC/MS.

Results and discussion

Electrochemical properties and catalysis of peroxide reduction of *Mro*APO on AuNP-CH/GCE

Immobilization of *Mro*APO on chitosan-capped gold nanoparticles is based on the electrostatic interaction between positively charged chitosan and the negatively charged enzyme. This hinders its leakage from the electrode surface.

Electrochemical properties of *Mro*APO modified sensors were investigated by using cyclic voltammetry and SWV. Cyclic voltammograms of *Mro*APO immobilized at the AuNP-CH-modified GCE displayed a pair of redox peaks at −239.6 m and −359.5 mV vs. Ag/AgCl (in 1 M KCl) at the scan rate of 1 V/s. *Mro*APO immobilized on pure chitosan-coated GCE without addition of AuNPs showed redox peaks with (about) 1.3 times smaller peak currents than in the presence of AuNPs. However, in the absence of *Mro*APO, both the bare GCE and the AuNP-CH-modified GCE showed no redox signal.

From the integration of the anodic peak, the surface coverage (Γ) of electrochemically active *Mro*APO (Γ=*Q*/nFA and A=7.07 mm^2) on AuNP-CH/GCE was determined to be at 20 mV/s, 26.5 pmol cm^{-2}. For a rough estimation of the surface concentration of a monolayer, the molecular size of chloroperoxidase (from *Caldariomyces fumago*) is considered because its molecular size is comparable [12]. The surface concentration of electro-active *Mro*APO on AuNP-CH/GCE reflects almost three completely covered electrode surfaces.

Thus the chitosan-coated AuNPs ensure electron transfer between the adsorbed enzyme and the electrode surface.

The formal potential ($E^{0\prime}$) of *Mro*APO in the gold nanoparticles-chitosan film was estimated to be −278.5 mV vs. Ag/AgCl (in 1 M KCl) at pH 7 by taking the midpoint of anodic and cathodic peak potentials. The formal potential is comparable to the previously published data for the Fe^{2+}/Fe^{3+}

redox couple of *Aae*APO (−286–9 mV vs. Ag/AgCl) [12] and other heme-thiolate enzymes [16–19].

SWV has been successfully applied for characterizing the heterogeneous electron transfer of proteins [20–22]. In Fig. 1 almost symmetric forward and backward SWVs of *Mro*APO-AuNP-CH/GCE are shown at an amplitude of 50 mV and a step size of 2 mV. The formal potential was determined to be −314 mV vs. Ag/AgCl (in 1 M KCl) which was close to the respective value from the cyclic voltammograms.

The heterogeneous electron transfer rate constants (k_s) of *Mro*APO adsorbed at the AuNP-CH/GCE were determined by the Laviron method [23] by using cyclic voltammetry. The k_s values increase from 3.7 s^{-1} to a saturation value of 17.47 s^{-1} in the scan rate range from 0.02 to 2.0 Vs^{-1}. For *Aae*APO a maximum value of k_s of 63.7 s^{-1} was reported [12]. The rise of the k_s with increasing scan rate indicates a surface-controlled electrochemical process.

In order to find the optimal concentration of hydrogen peroxide for the peroxide-dependent substrate conversion by *Mro*APO, cyclic voltammetry was used. Figure 2 shows the CVs of catalysis of peroxide reduction under aerobic conditions. Peak heights increased up to 50 μM and decreased above this concentration. Therefore, 50 μM was applied for investigations of substrate conversion.

Peroxide-dependent substrate conversion

The conversion of aniline into hydroxylaminobenzene and aminophenols represents two-electron oxidations associated with an oxygen transfer from the peroxide to the product (P450-like reaction). In contrast, the oxidation of phenolic substrates (hydroquinone, *p*-aminophenol, paracetamol, and resorcinol) is based on one-electron/hydrogen abstractions leading to reactive phenoxyl radicals that tend to couple and polymerize or to form benzoquinones and quinoneimines, respectively by disproportionation [24, 25]. The

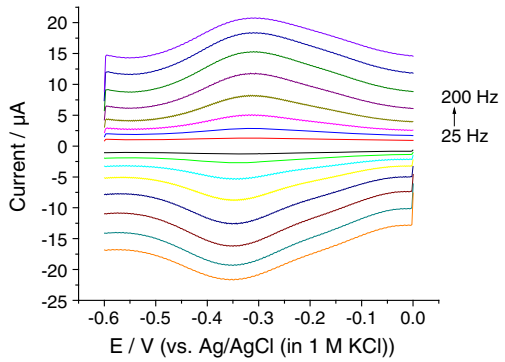

Fig. 1 SWVs of *Mro*APO-AuNP-CH/GCE at an amplitude of 50 mV and step size of 2 mV

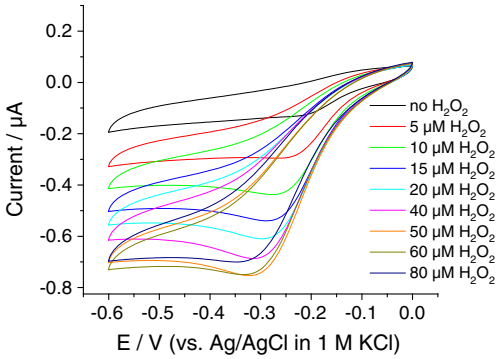

Fig. 2 CVs of *Mro*APO-AuNP-CH/GCE for different H_2O_2 concentrations, scan rate of 5 mV/s

oxidation of phenolic substrates in this way is a characteristic reaction of classic heme peroxidases.

In qualitative experiments done with limiting H_2O_2 amounts, we found that the *Mro*APO oxidized aniline, *p*-aminophenol, hydroquinone and paracetamol, releasing ring-hydroxylated, as well as quinoid intermediates and coupling products, which we identified by HPLC/MS. The mono-hydroxylated reaction products of the *Mro*APO-catalyzed oxidation of aniline were hydroxylaminobenzene (*N*-phenylhydroxylamine), *o*-aminophenol, and *p*-aminophenol. *p*-Aminophenol and paracetamol were oxidized to coupling products. For example, paracetamol $[M+H, 152]^+$ yielded a product with an *m/z* value of $[M+H, 318]^+$, which indicated the formation of a dimer. Hydroquinone was converted to *p*-benzoquinone as the major metabolite and other coupling products. Our attempts to identify the instable quinoneimines, which may have been formed during the *Mro*APO-catalyzed oxidation of aniline, *p*-aminophenol, and paracetamol, have not been successful.

Incubation of *p*-aminophenol with peroxide in the presence of *Mro*APO generated a product which could be reduced at 0 mV vs. Ag/AgCl (in 1 M KCl) at the bare GCE. The reduction current is attributed to the formation of quinoneimine. Obviously, the *Mro*APO-catalyzed reaction is distinct to the HRP-catalyzed reaction which generates a tetrameric final product which is reducible at −450 mV [26, 27]. Furthermore, we followed the *Mro*APO-catalyzed oxidation of *p*-aminophenol by measuring cyclic voltammograms between 0 and 400 mV vs. Ag/AgCl (in 1 M KCl) in order to characterize the stability of the oxidation product. The heights of the anodic peak at 182 mV vs. Ag/AgCl (in 1 M KCl) of *p*-aminophenol oxidation and of the corresponding cathodic peak at 61 mV vs. Ag/AgCl (in 1 M KCl) decreased within a reaction time of 20 min by only 12.9%. Therefore, the *Mro*APO-catalyzed oxidation of *p*-aminophenol results mostly in the formation of reaction products which are electro-active at the potential of the quinoneimine reduction. For the oxidation of hydroqui-

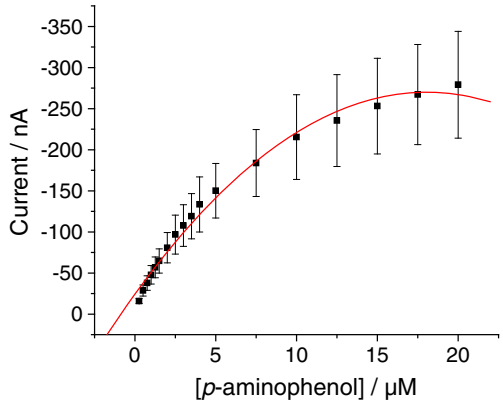

Fig. 3 Concentration dependence of the amperometric response for *p*-aminophenol in presence of 50 µM H_2O_2 (n=3). *Error bars* represent the standard error of the mean

none, the respective peaks decreased by almost 16.6% within a reaction time of 20 min.

Sensor development

Determination of total phenolic substrates is important both in environmental and drug analysis. In literature there are several reports describing the measurement of phenolic substances by using enzyme electrodes based on horseradish peroxidase, tyrosinase, laccase, other enzymes and tissue slides [24, 25, 28–42]. In order to investigate the potential of *Mro*APO, *p*-aminophenol, paracetamol, catechol, hydroquinone, resorcinol, and aniline were chosen as model substrates.

Sensors for phenolic substances

Figure 3 shows the sensor response on stepwise addition of pAP in presence of 50 µM peroxide at 0 mV vs. Ag/AgCl (in 1 M KCl) at pH 7. The current linearly increases between 0.25 and 5 µM with a lower limit of detection of 0.130 µM (S/N=3) and reaches saturation around 12 µM. There was no pronounced change in the currents between pH 7 and 8.

In the linear measuring range the *Mro*APO AuNP-CH/GCE yields for *p*-aminophenol a 1.38 times larger response than in the absence of gold nanoparticles. This difference most probably results from the structure difference between the two modified electrodes, as evidenced by SEM investigations [12].

In the chronoamperometric measurements with the *Mro*APO sensor, the reaction products are reduced back to the original substrate at the electrode thus competing with the formation of polymeric products. The electro-enzymatic recycling of the analyte proceeds at the total electro-active surface including the "contacted" AuNPs (Fig. 4).

Calibration graphs of six different substrates and analytical parameters are shown in Fig 5 and Table 1, respectively.

The highest sensitivities were found both for *p*-aminophenol and catechol, whilst currents in the linear range for paracetamol and hydroquinone were almost sixfold smaller. The lowest values were obtained for resorcinol. LODs are in the submicromolar region and are comparable with other monoenzyme sensors [29–33]. As described for the

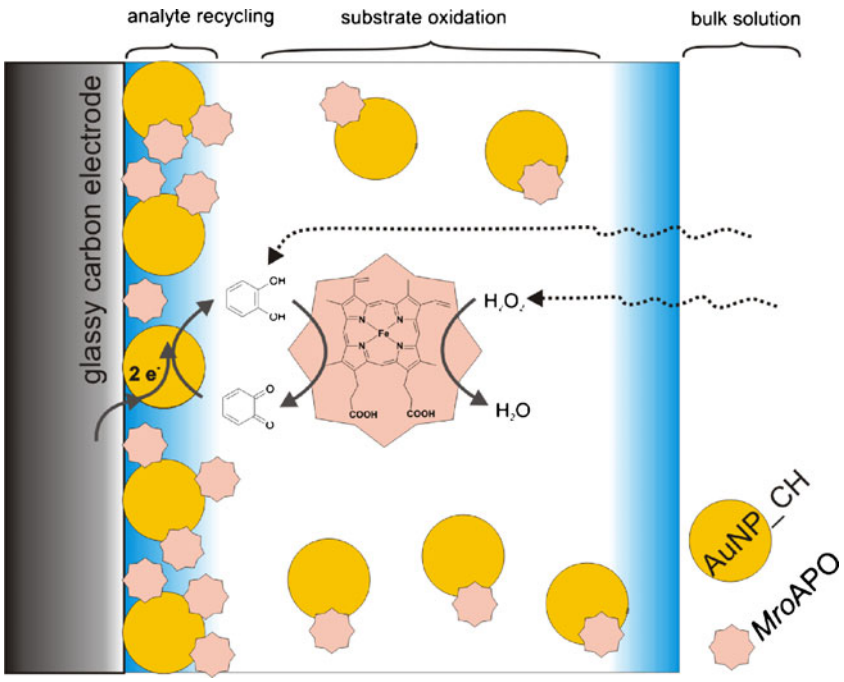

Fig. 4 Schematic representation of the electro-enzymatic recycling of a phenolic substrate (here, catechol) at the GC electrode covered by *Mro*APO immobilized in a matrix of chitosan embedded AuNPs. The chitosan coating is not shown

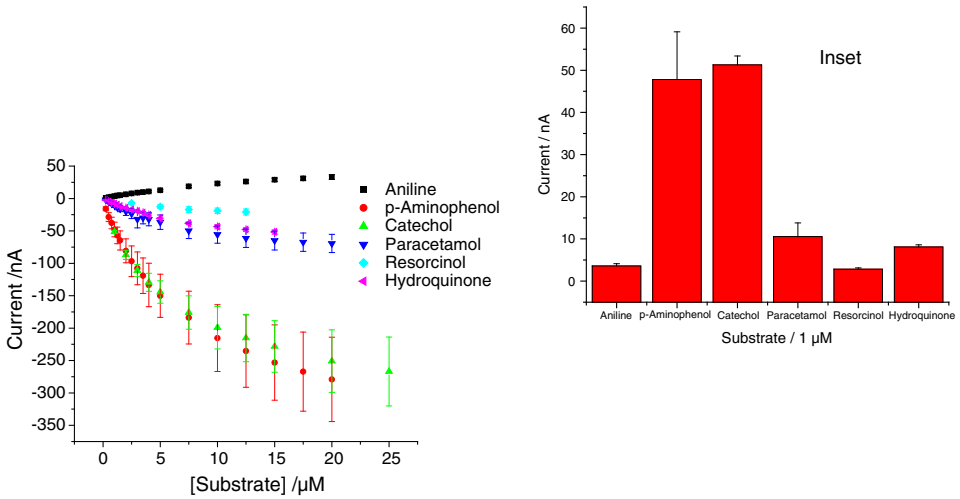

Fig. 5 Concentration dependencies and comparison of current at 1 µM for phenolic substances (at 0 V vs. Ag/AgCl (in 1 M KCl)) and aniline (at 0.2 V vs. Ag/AgCl (in 1 M KCl)) (n=3). Error bars represents the standard error of the mean

determination of phenolic compounds by a HRP-modified electrode, the sensitivity depends on the stability of phenoxy radicals formed in the enzymatic substrate conversion and the applied potential [25]. The radicals which are formed by the one-electron oxidation of catechol, hydroquinone, and *p*-aminophenol are stabilized by the formation of the conjugated structures. Therefore, the stronger the ability of electron-donor conjugation of a substituent, the higher the sensitivity for the substrate. On the other hand, the *m*-hydroxy group of resorcinol will not stabilize the radicalic structure. Due to the effective polymerisation reaction the sensitivity for resorcinol should be low.

Aniline hydroxylation

The catalytic potential of *Mro*APO to hydroxylate aromatic substances was exploited to generate the amperometric signal for detecting aniline in the presence of H_2O_2. Figure 6 shows the amperometric response of *Mro*APO-AuNP-CH/GCE at 200 mV vs. Ag/AgCl (in 1 M KCl) on stepwise addition of aniline in the presence of 50 µM H_2O_2. Whilst in the presence of H_2O_2 there is an increase in the anodic current indicating formation of *p*-aminophenol, in the absence no signal can be detected (data not shown). As seen from the inset in Fig 6, the catalytic current linearly increases with increasing aniline concentration in the range from 0.25 to 10 µM with a regression factor of 0.9957.

For immobilized *Mro*APO, a starting activity of 2 units/cm^2 (for the standard substrate veratryl alcohol) was applied. The activity for the aromatic hydroxylation was almost sixfold lower [11]. Therefore, the sensor response for aniline is limited by the rate of enzyme reaction (kinetic control regime). In accordance with the low enzyme activity, the concentration dependence for aniline follows the Michaelis–Menten equation. Furthermore, the low peroxide concentrations decrease the linear measuring range. The currents in the linear measuring range and at saturation for *p*-aminophenol are bigger than for aniline (Fig. 6). This behavior reflects the higher activity towards phenolic compounds as compared with the hydroxylation of aniline.

In addition to the stability of the radicals generated in the peroxide-dependent enzyme catalysis the specificity of the

Table 1 Analytical parameters of *Mro*APO-AuNP-CH/GCE for six substrates

Substrate	Linear range (µM)	R^2	LOD (µM) (S/N=3)	Current/1 µM substrate (nA/µM)
Aniline	0.25–5	0.9957	0.160	3.5875
p-Aminophenol	0.25–5	0.9916	0.130	−47.8
Catechol	1–10	0.9712	0.109	−51.2667
Paracetamol	0.25–2.5	0.9963	0.182	−10.55
Resorcinol	2.5–12.5	0.9698	0.156	−2.82
Hydroquinone	0.25–5	0.9973	0.101	−8.1
L-DOPA	–		–	–
p-Nitrophenol	–		–	–

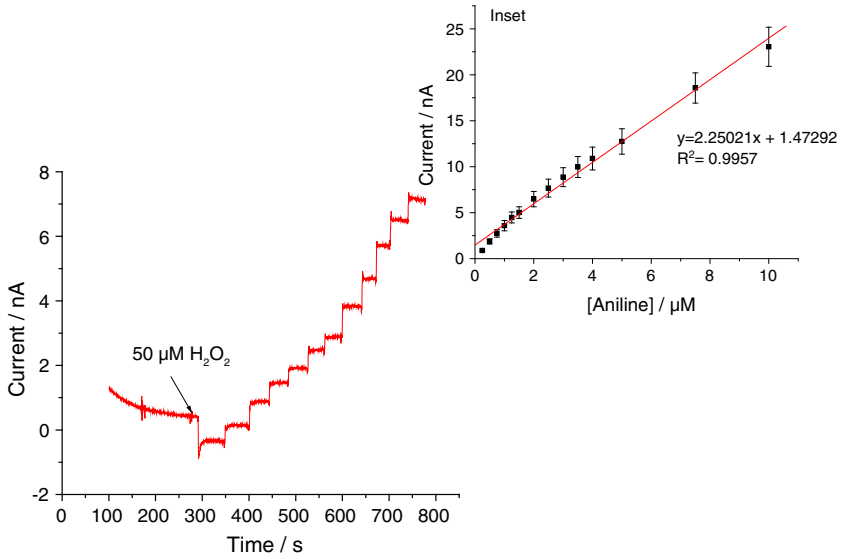

Fig. 6 Amperometric response of *Mro*APO-AuNP-CH/GCE on stepwise addition of six times 0.25 µM and five times 0.5 µM aniline in the presence of 50 µM H_2O_2 at 200 mV. *Inset*, linear measuring range for aniline (n=3)

biocatalyst dictates the rate of formation of electrode-active products and thus the relative sensitivities of a series of phenolic compounds. The *Aae*APO sensor exhibited almost identical sensitivity for *p*-aminophenol as compared with aniline but did not generate a reduction current for catechol. Using the same enzyme loading, the enzyme electrode based on *Mro*APO exhibits almost identical sensitivity for aniline as the *Aae*APO sensor. However, the slope of the linear part of the calibration curve for *p*-aminophenol is almost ten times higher. Therefore, the limit of detection for pAP and other phenolic substances of the *Mro*APO sensor is lower. These results obtained for identical activities of both peroxygenases for the standard substrate veratrylalcohol show that *Mro*APO exhibits a higher peroxidatic activity as compared with *Aae*APO. On the other hand, the activity of *Mro*APO toward L-DOPA and *p*-nitrophenol is not sufficient for the efficient generation of the electroactive hydroxylated products. Therefore, a sensor containing both peroxygenases should posses a broad spectrum of measurable analytes.

For a sensor using microperoxidase in the same immobilization matrix, we obtained for *p*-aminophenol and catechol almost identical sensitivities which were in the linear range twofold and at saturation 12-fold higher than for aniline. No response toward *p*-nitrophenol was found [43]. The relative sensitivities of the enzyme electrode based on the *Mro*APO -catalyzed substrate oxidation presented in this paper shows a very similar pattern (Fig. 5). For HRP entrapped in an alumina nanoparticle-chitosan layer [38] or a layer by layer electrode [25] the signals for catechol and hydroquinone are almost four times higher than for resorcinol and phenol and no response was found for *p*-nitrophenol. A very similar pattern for phenolic substances has been reported by Kubota et al. [37] for HRP entrapped in an inorganic sol–gel support whilst Smyth [24] found a quite different substrate spectrum for HRP with cumene hydroperoxide as a cosubstrate.

Conclusions

*Mro*APO has the potential to act as recognition element in enzyme electrodes in addition to the applications in metabolic reactors. Its peroxidatic activity for the oxidation of phenolic compounds shows a similar substrate spectrum as HRP. The P450 analogous activity which is almost one order of magnitude lower is sufficient for aniline detection, but not for *p*-nitrophenol.

On the other hand, the *Aae*APO sensor allows the measurements of several aromatic substances, e.g., *p*-nitrophenol and may also be extended to real drugs. However typical substrates of plant peroxidases, e.g., catechols and catecholamines, are not converted with comparable rates.

The following new sensor principles might be derived from the results presented:

- The coimmobilisation of *Mro*APO and *Aae*APO will result in a sensor with a very broad spectrum of analytes.
- The stability of *Mro*APO in non-aqueous solvents [11] will allow for the measurement of water-insoluble phenolic substances.
- To create substrate specific sensors, interfering sample constituents can be removed by co-immobilized enzymes.

Acknowledgments The authors gratefully acknowledge the financial support of BMBF (0311993) of Germany. This work is a part of UniCat, the Cluster of Excellence in the field of catalysis coordinated by TU Berlin and financially supported by Deutsche Forschungsgemeinschaft within the framework of the German Excellence Initiative (EXC 314).

References

1. Gauglitz G (2010) Anal Bioanal Chem 398:2363–2372
2. Renneberg R (2009) Bioanalytik für Einsteiger. Spektrum Akademischer Verlag, Heidelberg
3. Heller A, Feldman B (2008) Chem Rev 108:2482–2505
4. Renneberg R, Lisdat F (2008) Advances in biochemical engineering/biotechnology, vol 109. Springer, Berlin
5. Willner I, Katz E (2005) Bioelectronics. Wiley, Weinheim
6. Wollenberger U, Renneberg R, Bier F, Scheller F (2003) Analytische Biochemie-Eine praktische Einführung in das Messen mit Biomolekülen. Wiley, Weinheim
7. Joo H, Lin Z, Arnold FH (1999) Nature 399:670–673
8. Hofrichter M, Ullrich R (2010) New trends in fungal biooxidation. The Mycota,volume X, industrial applications, 2nd edn. Springer, Berlin
9. Torres E, Ayala M (2010) Biocatalysis based on heme peroxidases: peroxidases as potential industrial biocatalysts. Springer, Berlin
10. Hofrichter M, Ullrich R, Pecyna MCL, Lundell T (2010) Appl Microbiol Biotechnol 87:871–897
11. Gröbe G, Ulrich R, Pecyna M, Friedrich S, Hofrichter M, Schreibner K (2011) AMB Express 1:31
12. Peng L, Wollenberger U, Kinne M, Hofrichter M, Ulrich R, Schreibner K, Fischer A, Scheller FW (2010) Biosens Bioelectron 26:1432–1436
13. Ullrich R, Nuske J, Scheibner K, Spantzel J, Hofrichter M (2004) Appl Environ Microbiol 70:4575–4581
14. Bonnard C, Papermaster DS, Kiraehenbuhl J-P (1984) The streptavidin-biotin bridge technique: applications in light and electron microscope immunocytochemistry. In: Polak JM, Varndell IM (eds) Immunolabeling for electron microscopy. Elsevier, New York
15. Yarman A, Nagel T, Gajovic-Eichelmann N, Fischer A, Wollenberger U, Scheller FW (2011) Electroanalysis 23:611–618
16. Bistolas N, Wollenberger U, Jung C, Scheller FW (2005) Biosens Bioelectron 20:2408–2423
17. Mak LH, Sadeghi SJ, Fantuzzi A, Gilardi G (2010) Anal Chem 82:5357–5362
18. Shumyantseva VV, Bulko TV, Kumetsova GP, Lisitsa AV, Ponomarenko EA, Karuzina II, Archakov AI (2007) Biochem Mosc 72:658–663
19. Krishnan S, Wasalathanthri D, Zhao LL, Schenkman JB, Rusling JF (2011) JACS 133:1459–1465
20. Osteryoung JG, Osteryoung RA (1985) Anal Chem 57:101A–106A
21. Zhang Z, Nassar A-EF, Lu Z, Schenkman JB, Rusling JF (1997) J Chem Soc, Faraday Trans 93:1769–1774
22. Jeuken LJC, McEvoy JP, Armstrong FA (2002) J Phys Chem B 106:2304–2313
23. Laviron E (1979) J Electroanal Chem 101:19–28
24. Kane SA, Iwuoha EI, Smyth MR (1998) Analyst 123:2001–2006
25. Yang S, Li Y, Jiang X, Chen Z, Lin X (2006) Sens Actuators B 114:774–780
26. Sun W, Jiao K, Zhang S, Zhang C, Zhang H (2001) Anal Chim Acta 434:43–50
27. Zhang S, Jiao K, Chen H (1999) Anal Lett 32:1761–1773
28. Wollenberger U, Lisdat F, Rose A, Streffer K (2008) Bioelectrochemistry: fundamentals, experimental techniques and applications. Wiley, New York
29. Munteanu FD, Lindgren A, Emnéus J, Gorton L, Ruzgas T, Csöregi E, Ciucu A, van Huystee RB, Gazaryan IG, Lagrimini LM (1998) Anal Chem 70:2596–2600
30. González-Sánchez MI, Rubio-Retama J, López-Cabarcos E, Valero E (2011) Biosens Bioelectron 26:1883–1889
31. Ameer Q, Adeloju SB (2009) Sens Actuators B 140:5–11
32. Topcu Sulak M, Erhan E, Keskinler B (2010) Appl Biochem Biotechnol 160:856–867
33. Erdem A, Pabuccuoglu A, Meric B, Kerman K, Ozsoz M (2000) Turk J Med Sci 30:349–354
34. Marko-Varga G, Emnéus J, Gorton L, Ruzgas T (1999) TrAC Trends Anal Chem 14:319–328
35. Zhang Y, Zeng GM, Tang L, Huang DL, Jiang XY, Chen YN (2007) Biosens Bioelectron 22:2121–2126
36. Tan Y, Guo X, Zhang J, Kan J (2010) Biosens Bioelectron 25:1681–1687
37. Rosatto SS, Sotomayor PT, Kubota LT (2002) Gushikem Y 47:4451–4458
38. Liu X, Luo L, Ding Y, Xu Y (2011) Analyst 136:696–701
39. Serra B, Benito B, Agüí L, Reviejo AJ, Pingarrón JM (2001) Electroanalysis 13:693–700
40. Topcu S, Sezginturk MT, Dinckaya E (2004) Biosens Bioelectron 20:592–597
41. Navaratne A, Lin MS, Rechnitz GA (1990) Anal Chim Acta 237:107–113
42. Fatibello-Filho O, Lupetti KO, Vieira IC (2001) Talanta 55:685–692
43. Yarman A, Badalyan A, Gajovic-Eichelmann N, Wollenberger U, Scheller FW Biosens Bioelectron (in press) doi:10.1016/j.bios.2011.09.004